http://dx.doi.org/10.5935/0103-5053.20160096

J. Braz. Chem. Soc., Vol. 27, No. 11, 2062-2069, 2016.
Printed in Brazil - ©2016 Sociedade Brasileira de Química
0103 - 5053 $6.00+0.00

Article

The Effect of Gamma-Al_2O_3 Support on the NO Adsorption on Pd_4 Cluster

Letícia M. Prates,[a] Glaucio B. Ferreira,[b] José W. M. Carneiro,[b] Wagner B. de Almeida,[b]
Alexandre N. M. Carauta,[c] Julio C. G. Correia[d] and Maurício T. M. Cruz*,[a]

[a]*Departamento de Química Geral e Inorgânica, Instituto de Química, Universidade do Estado do Rio de Janeiro, Campus Maracanã, 20550-900 Rio de Janeiro-RJ, Brazil*

[b]*Departamento de Química Inorgânica, Instituto de Química, Universidade Federal Fluminense, Campus do Valonguinho, 24020-141 Niterói-RJ, Brazil*

[c]*Fundação Técnico-Educacional Souza Marques, 21310-310 Rio de Janeiro-RJ, Brazil*

[d]*Centro de Tecnologia Mineral, Avenida Pedro Calmon, 900, 21941-908 Rio de Janeiro-RJ, Brazil*

The effect of γ-Al_2O_3 support on the NO adsorption on Pd_4 clusters was investigated by means of density functional theory (DFT) calculations. Pd_4 adsorbed on γ-Al_2O_3 (represented by a $Al_{14}O_{24}H_6$ cluster) changes its preferential geometry from tetrahedral to a distorted planar structure. The alumina support promotes a higher dispersion in the palladium catalyst and reduces the NO adsorption energy to –25.6 kcal mol^{-1} (computed at B3LYP/LANL2DZ/6-311+G(d)), in close agreement with the experimental value of –27.2 kcal mol^{-1}. On the bare planar Pd_4 cluster the NO molecule adsorbs in a bridge arrangement, with adsorption energy of –41.2 kcal mol^{-1}. Adsorption on the tetrahedral Pd_4 cluster occur preferentially in an atop mode, with adsorption energy of –30.6 kcal mol^{-1}. Charge density analysis show that the electron flux between the NO molecule and Pd_4 depends on the adsorption form, with back-donation being stronger in the bridge adsorption mode.

Keywords: Pd clusters, DFT, supported-Pd clusters, alumina, NO adsorption, back-donation

Introduction

Palladium catalysts have found wide appllication in several areas of chemistry.[1-3] One of the most common and established use of palladium catalyst is to control automobile exhaust gas emission.[4-6] Use of catalytic converter in automobile exhaust is a requirement to reach the recommended limits for emission of toxic byproducts. Although studies have been dedicated to the understanding of the catalytic conversion process in the exhaust emission,[7] more fundamental studies are still necessary for a full comprehension of the catalytic process, particularly at the molecular level.[8,9]

Commonly, the platinum and palladium catalysts are supported on metal oxides, among them γ-Al_2O_3, although oxides of cerium, zirconium and titanium are also frequently employed.[10-12] These supported catalysts are thus employed to remove carbon monoxide (CO), nitric oxide (NO), NO_x and SO_x contaminants, among others, from the exhaust engine.[4-6]

Nitric oxide has an odd number of electrons and is one of the most versatile molecules, making its chemistry and adsorption process of particular interest.[13] The adsorption of NO on the supported catalyst surface has been investigated by both experimental[7,14-20] and theoretical procedures.[21-29] NO adsorbs on small Pd clusters through its nitrogen atom in a tilted orientation, preferentially in the hcp threefold and bridge sites,[27] although the relative binding energies are strongly dependent on the size and geometry of the cluster employed.[27] For adsorption of NO on an extended surface at low coverage the interaction is determined by electron donation and back-donation involving the 5σ/2π* antibonding orbital of the NO molecule and the d-bands of the transition metal, with a net charge transfer from the transition metal to the adsorbed NO.[29] However, the extent of the interaction via the back-donation process is strongly dependent on the coordination mode of the NO molecule. On a flat surface, the preferential adsorption occurs on a hollow-site.[29] Adsorption on the energetically less favorable top-site results in tilted orientation with the NO bent to the metal surface.

In the vast literature on theoretical studies of NO adsorption on metal surfaces, the catalyst is frequently represented as a single crystal[29] or as a small atomic cluster,[21-24,27,28] although evidence shows that the support

---

*e-mail: cruzmtm@uerj.br

plays a relevant role in the reactivity of the supported catalyst.[10-12,18-20,25,26] The oxidation of Pd nanoparticles is improved in the presence of the γ-Al_2O_3 support.[30,31]

In the supported catalyst, the size of the metal particles may vary to some degree. Dispersed clusters are usually formed by small number of atoms. Extended X-ray absorption fine structure (EXAFS) analysis of a fresh platinum catalyst supported on Al_2O_3 indicated an average Pt–Pt coordination number of 2.6 ± 0.4, suggesting a platinum cluster size of 3 to 4 atoms dispersed on the γ-alumina surface.[32] Therefore, simulation with a small cluster of atoms considering the presence of the support should grasp the main features of the real system.

The structure of γ-Al_2O_3 is characterized by the presence of tetrahedral and octahedral aluminum atoms. In a study employing density functional theory (DFT) to compute the adsorption of formaldehyde on palladium supported on γ-Al_2O_3 we showed that the Pd–Al_2O_3 interactions result in charge transfer from octahedral aluminum atoms to the deposited Pd cluster.[33] The tetrahedral aluminum site has high acididity, acting as electron acceptors, while octahedral aluminum sites act as electron donors.[33] Therefore, it was possible to establish the electron flux between the γ-Al_2O_3 support and the metal cluster.

In the present study we return to the discussion on the the adsorption properties of small palladium clusters supported on γ-Al_2O_3. We employed the DFT B3LYP approach to analyze the energies for adsorption of nitric oxide on a Pd_4 cluster supported on a model for γ-Al_2O_3. The goal was to quantify geometric, electronic and energetic parameters involved in the adsorption of NO on the palladium clusters and evaluate the effect of the support γ-Al_2O_3 on the adsorption process.

Methodology

In the present work we report data for adsorption of NO (Figure 1a) on planar (Figure 1b) and tetrahedral (Figure 1c) Pd_4 clusters and on the Pd_4 cluster supported on a model for the (110) surface of γ-Al_2O_3 (Figure 1d).

The model for the γ-Al_2O_3 surface was obtained from the unit cell of γ-Al_2O_3 by cutting a slice in the (110) direction of the unit cell. The resulting surface exposes both tetrahedral and octahedral aluminum atoms, as

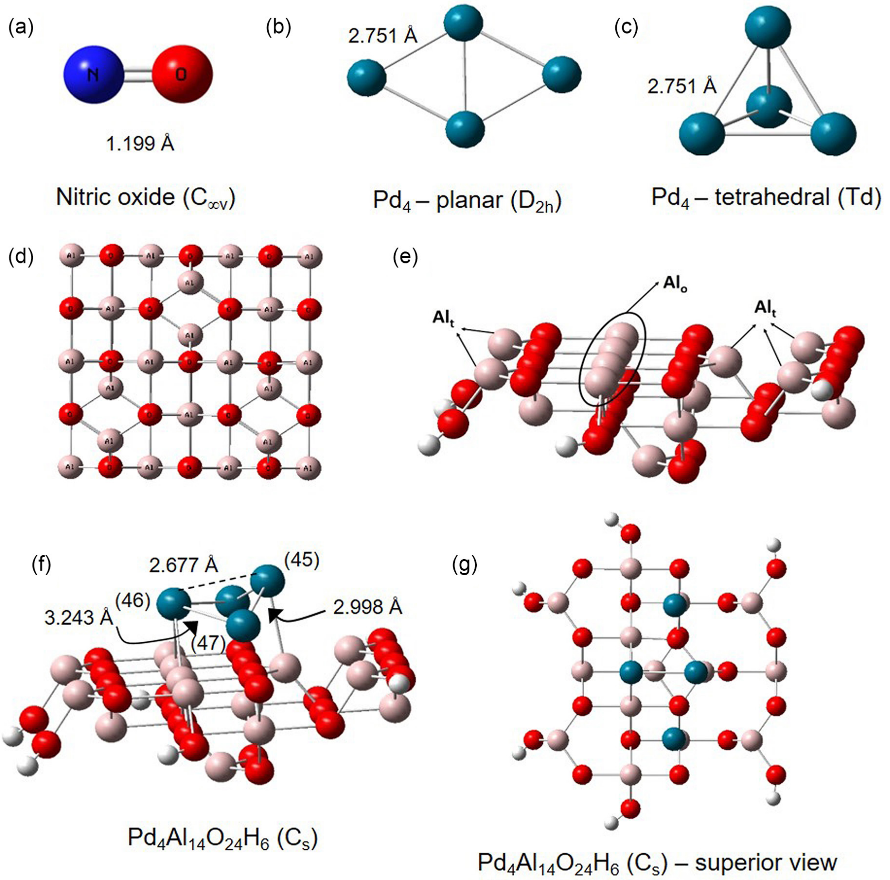

Nitric oxide ($C_{\infty v}$)

Pd_4 – planar (D_{2h})

Pd_4 – tetrahedral (Td)

$Pd_4Al_{14}O_{24}H_6$ (C_s)

$Pd_4Al_{14}O_{24}H_6$ (C_s) – superior view

Figure 1. Structures of the (a) nitric oxide (NO) molecule; (b) planar Pd_4 cluster; (c) tetrahedral Pd_4 cluster; (d) general representation of γ-Al_2O_3; (e) $Al_{14}O_{24}H_6$ unit used to represent the γ-Al_2O_3 support; and (f) lateral and (g) superior views of Pd_4 optimized over the $Al_{14}O_{24}H_6$ unit. Distances are given in Å, Al_t is for tetrahedral aluminum atoms and Al_o is for octahedral aluminum atoms.

well as oxide anions, to external interactions, in addition to being the most stable face for γ-alumina.[34,35] Due to computational cost, the γ-Al_2O_3 model was restricted to three sheets of atoms containing a total of 14 aluminum and 24 oxygen atoms. To balance charge and yield a neutral model, 6 hydrogen atoms were added to terminal oxygens, leading to a final model with $Al_{14}O_{24}H_6$ stoichiometry. In the γ-Al_2O_3 model, each oxygen atom is coordinated to at least two aluminum (or one aluminum and a hydrogen, in the case of the terminal oxygen atoms) and each aluminum is coordinated to at least three oxygen atoms, therefore reducing any border effect. Experimental distances and angles were used to construct the γ-Al_2O_3 model.[36]

On the (110) face of the γ-alumina we deposited the Pd_4 cluster, starting from a planar geometry for the Pd_4 moiety and Pd–Pd distances of 2.751 Å (Figure 1b), with the palladium atoms interacting with both tetrahedral and octahedral aluminum atoms. The Pd_4 cluster was then optimized on the γ-Al_2O_3 surface, leading to a distorted geometry (Figures 1f and 1g). Considering that tetrahedral Pd_4 cluster has a triplet ground state[33] and that the γ-Al_2O_3 model has a singlet ground state,[37] all calculation involving the Pd_4 deposited on the γ-Al_2O_3 was carried out in the total triplet electronic state, using the unrestricted formalism (see Table S1). For all unrestricted calculations the stability of the final wave function was tested and the adsorption energies were computed using the most stable wave function in each case.

After having prepared the Pd_4/γ-Al_2O_3 aggregate for adsorption, the NO molecule was optimized in several orientations over the $Pd_4/Al_{14}O_{24}H_6$ cluster. Initially, the calculations were performed relaxing only the NO distance and orientation, while keeping the positions of the atoms in the $Pd_4/Al_{14}O_{24}H_6$ cluster in their original positions. In the final step, both the NO molecule and the Pd_4 unit were allowed to relax.

To have a reference for the effect of the γ-alumina surface on the NO adsorption energy, we also computed the NO adsorption on a naked Pd_4 cluster. The NO molecule was optimized on the following three clusters, all containing four palladium atoms, each in different arrangements: (*i*) the planar arrangement in D_{2h} rhombohedral symmetry (Figure 1b); (*ii*) the tetrahedral arrangement with T_d symmetry (Figure 1c); and (*iii*) the distorted arrangement obtained in the previous optimization of Pd_4 on the $Al_{14}O_{24}H_6$ cluster. In these cases only the NO molecule was allowed to relax during the optimization process, whereas the palladium atoms were kept fixed in their original positions. Several adsorption modes for the NO molecule on Pd_4 were simulated: atop, bridge, hollow, di-σ and π, as shown in Figure 2. When possible, symmetry was imposed.

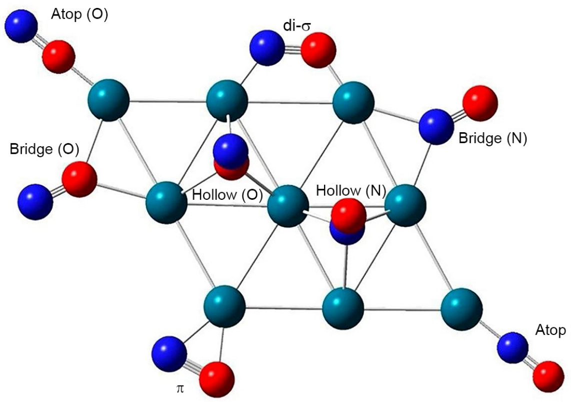

Figure 2. Different positions for adsorption of nitric oxide on the palladium (111) surface. Atop (O) and atop (N) are for adsorption of NO on a specific palladium atom, via the oxygen or the nitrogen atom, respectively. Bridge (O) and bridge (N) are for adsorption of NO on a bridge position, via the oxygen or the nitrogen atom, respectively. Hollow (O) and hollow (N) are for NO adsorption on the hollow positions, via the oxygen or the nitrogen atom, respectively. Di-σ and π are for adsorption in parallel orientations, as shown in the figure.

The NO adsorption energies were computed by summing the energies of the NO molecule and of the Pd_4 or $Pd_4/Al_{14}O_{24}H_6$ cluster and subtracting the result from the energy of the NO/Pd_4 or NO/$Pd_4/Al_{14}O_{24}H_6$ complex, according to equation 1.

$$E_{ad} = E_{(NO/Pd_4/Al_{14}O_{24}H_6)} - \left[E_{(NO)} + E_{(Pd_4/Al_{14}O_{24}H_6)}\right] \quad (1)$$

The adsorption energies were subjected to correction due to the basis set superposition error (BSSE),[38,39] using equations 2 and 3.

$$E_{ad/corr.} = E_{(AB)} - \left[E_{(A\cancel{B})} + E_{(\cancel{A}B)} + \left(-E_{def}\right)\right] \quad (2)$$

$$E_{def} = E_{B(AB)} - E_{(B)} \quad (3)$$

In these equations $E_{ad/corr.}$ is the BSSE corrected adsorption energy; A is the cluster (Pd_4 or $Pd_4/Al_{14}O_{24}H_6$) and B is the NO molecule; $E_{(AB)}$ is the energy of the NO/Pd_4 or the NO/$Pd_4/Al_{14}O_{24}H_6$ complexes; $E_{(A\cancel{B})}$ and $E_{(\cancel{A}B)}$ are the absolute energies of the NO/Pd_4 or the NO/$Pd_4/Al_{14}O_{24}H_6$ complexes, considering the nuclei of B and A, respectively, as absent; E_{def} is the deformation energy of NO, computed from the difference in the energy of NO in the geometry of the complex ($E_{B(AB)}$) and in the fully optimized geometry ($E_{(B)}$).

All calculations were carried out using the Gaussian 03 computational package,[40] with the B3LYP hybrid functional as proposed and parameterized by Becke.[41] This is a mixture of Hartree-Fock and DFT exchange terms with the gradient-corrected correlation functional of Lee *et al.*[42] The palladium atoms and the γ-alumina atoms were described by the LANL2DZ pseudopotential[43] and the D95V[44] basis set for the valence electrons. The NO molecule was described by the 6-311+G(d) basis set.[45]

Charge densities were computed using the natural bond orbital (NBO) approach, to identify the main electron flux between the several units interacting in the NO/Pd_4, $Pd_4/Al_{14}O_{24}H_6$ and NO/$Pd_4/Al_{14}O_{24}H_6$ complexes.

Results and Discussion

Adsorption of NO on Pd_4 clusters

The preferential site for adsorption of NO on Pd_n cluster seems to have not yet been defined precisely. Recent studies proposed adsorption either on the atop[21] or on the hollow and bridge sites,[46] following previous computational studies that also suggested threefold hollow[47] or threefold hollow plus atop sites as the preferential adsorption mode.[48]

In the present study, we computed the adsorption of NO on three different Pd_4 clusters, planar (Figure 1b), tetrahedral (Figure 1c) and the distorted cluster obtained after optimization of Pd_4 over the γ-alumina surface (Figures 1f and 1g). Several electronic spin states were considered, using either the restricted (singlet) or the unrestricted (doublet to septet states) formalisms. It has been shown[49] that the ground electronic state for small Pd_7 and Pd_{10} clusters have triplet (S = 1) and septet (S = 3) spin states, respectively. For the Pd_4 cluster in any of the three arrangements computed, we found the triplet as the ground state, with the tetrahedral arrangement always more stable than the corresponding planar form. The distorted arrangement is less stable than tetrahedral and planar palladium clusters.

We computed the several alternatives for interaction between the NO molecule and Pd_4, as shown in Figure 3. The most stable form for adsorption of NO on planar Pd_4 is on the bridge site, with adsorption energy of –41.2 kcal mol^{-1} (Table 1), followed by adsorption on the hollow, atop 1 and atop 2 sites, which have adsorption energies lower by 3.2, 8.5 and 11.1 kcal mol^{-1}, respectively (Figures 3a-3d). On the tetrahedral Pd_4 cluster (Figures 3e-3g) the atop adsorption site is preferential, with adsorption energy of –30.6 kcal mol^{-1}, followed by adsorption on the bridge and hollow sites, with adsorption energy lower by 1.4 and 9.6 kcal mol^{-1}, respectively (Table 1). The energy for atop adsorption on the distorted arrangement of Pd_4 (the only adsorption mode found for supported Pd_4) is –31.8 kcal mol^{-1}, in the midway between atop adsorptions on the tetrahedral and on the planar arrangements. Therefore, the preferential adsorption site is dependent on the arrangement of the Pd_n cluster, as found in previous studies,[22,23,50] with palladium atoms having higher coordination number showing lower ability to accept the NO molecule.

Adsorptions on the atop sites lead to Pd–N distances that are in general lower than the corresponding Pd–N distances for adsorption on the bridge or hollow sites, reflecting the lower coordination number of the adsorbed NO molecule. In any case, the adsorption occurs in a tilted orientation, with O–N–Pd angles between 113 and 136°. The higher tilting was found for the bridge modes.

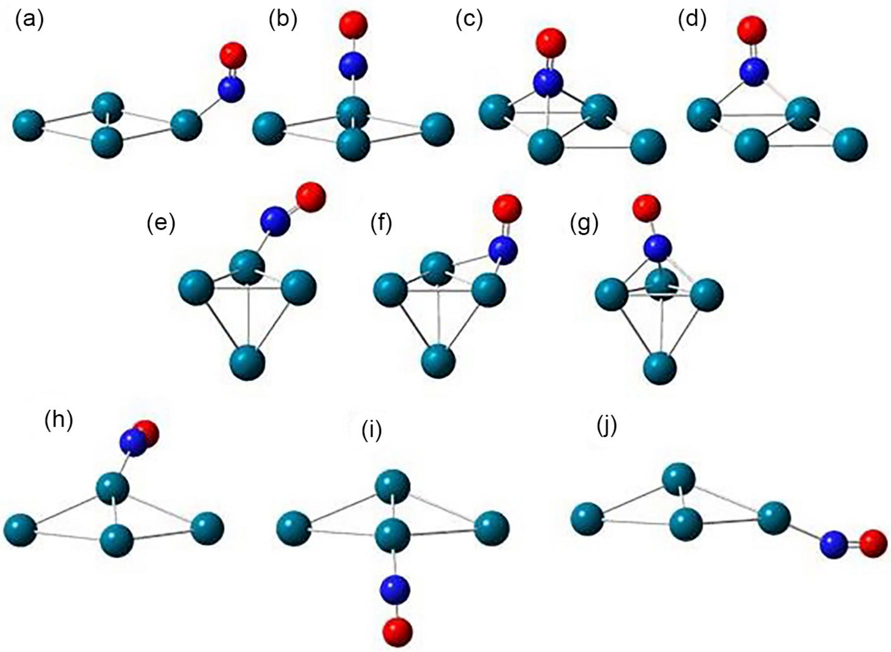

Figure 3. Different arrangements for adsorption of NO on planar, tetrahedral and distorted Pd_4 clusters.

Table 1. Adsorption energy (E_{ad}, kcal mol^{-1}, corrected for BSSE), charge density (e^-) on Pd_4 and selected geometrical parameters for nitric oxide adsorbed on planar and on tetrahedral Pd_4 (distances in Å and bond angles in degrees)

Form	Pd_4 (planar, D_{2h})				Pd_4 (tetrahedral, Td)		
	Atop (1) (A)	Atop (2) (B)	Bridge (C)	Hollow (D)	Atop (E)	Bridge (F)	Hollow (G)
N–Pd / Å	1.831	1.857	1.964	1.976	1.836	2.016	1.987
O–N–Pd / degree	135.00	129.43	121.68	125.25	135.68	113.52	119.13
N–O / Å	1.152	1.156	1.180	1.200	1.157	1.191	1.204
q_t (Pd_4) / e^-	–0.096	–0.111	+0.031	+0.167	–0.036	+0.176	+0.093
$E_{ad.}$ / (kcal mol^{-1})	–32.68	–30.65	–41.22	–38.01	–30.57	–29.20	–21.02

q_t: charge density; $E_{ad.}$: adsorption energy.

One important point is the electron flux between the two moieties. This is also a parameter which depends on the adsorption site. Previous studies reported that the NO adsorption process happens with charge back-donation from the Pd_4 cluster to the NO molecule.[21] Our results indicate that the amount of charge transferred between the two moieties depends on the adsorption site, but not on the arrangement. In both arrangements, adsorption in the atop mode, where back-donation to the $2\pi^*$ orbital of NO seems to be less efficient, results in charge transfer from the NO molecule to the Pd_4 cluster, while for adsorption in the bridge and hollow modes, charge is transferred from the Pd_4 cluster to the NO molecule. As a consequence, the NO distances in the NO adsorbed on the bridge or hollow sites are larger than those for the NO adsorbed on the atop sites. This should have consequences for the NO reduction process and, therefore, for the catalyst efficiency.

In summary, our computations for adsorption of NO on Pd_4 show that adsorption energies and preferential adsorption mode are strongly dependent on the arrangement of the Pd_n cluster, in agreement with previous studies.[22,23] In spite of these facts, the general trends are that adsorption on palladium atoms with higher coordination number results in lower adsorption energies and the back-donation is less efficient for adsorption on atop sites.

The $Pd_4/Al_{14}O_{24}H_6$ cluster

Starting from a planar arrangement with palladium atoms interacting with both tetrahedral and octahedral aluminum atoms, Pd_4 was fully optimized on the $Al_{14}O_{24}H_6$ cluster, while keeping the $Al_{14}O_{24}H_6$ moiety unchanged. The final optimized geometry for Pd_4 resembles one intermediate between the planar and the tetrahedral arrangements (Figures 1f and 1g). In a previous study on the adsorption of Pd_4 on the surface of α-Al_2O_3(0001),[51] the arrangement of the Pd_4 cluster that resulted in the highest adsorption energy is similar to the almost flat arrangement we found in the present case. Palladium atoms interact with both aluminum (tetrahedral and octahedral) and oxygen atoms. Three of the four palladium atoms adsorb in bridge positions, between either two octahedral aluminum or two oxygen atoms. The fourth one assumes an atop position over a tetrahedral aluminum atom. In general, the positions of the palladium atoms are close to the vacant sites of the alumina framework (Figures 1f and 1g).

After adsorption on the support, the palladium atoms become more dispersed than in the isolated cluster, with the peripheral atoms showing elongated Pd–Pd distances, while the central Pd–Pd distance is decreased (Figure 1f). On average, the peripheral Pd–Pd distances in the supported Pd_4 are 2.975 Å, as compared to 2.751 Å in bulk palladium. One of the central Pd–Pd distances becomes shorter (2.677 Å) than in the bulk palladium.

The smallest Pd–O distances are 2.160 and 2.206 Å, while the smallest Pd–Al distances are 2.527 and 2.616 Å. Among all Pd–Al distances in the metal-alumina interface, those distances involving the octahedral aluminum atoms (Al_o) are shorter than the distances involving the tetrahedral aluminum atoms (Al_t). Therefore, although one of the palladium atoms sits atop on a tetrahedral aluminum atom, the Pd–Al_t distance is larger than for the Pd–Al_o case, where the palladium atoms are adsorbed on a site between two aluminum atoms.

The strong distortion promoted upon adsorption of Pd_4 on the alumina support is a consequence of the strong interaction between the two subunities. The energy for adsorption of Pd_4 on the alumina support is 197.7 kcal mol^{-1}. If we add to this the energy necessary to distort the Pd_4 cluster from the planar arrangement to the arrangement it has on the alumina surface (18.7 kcal mol^{-1}), it results that the total interaction energy between the Pd_4 and the alumina surface is 216.4 kcal mol^{-1}.

The total NBO atomic charge on the Pd_4 unit adsorbed on the alumina surface is positive (0.475 e^-), concentrated on the palladium atoms adsorbed in bridge positions over oxygen atoms (Pd(47) and Pd(48), Figure 1f). When the palladium atom is adsorbed bridge on the octahedral aluminum (Pd(46)) or atop on the tetrahedral aluminum (Pd(45)) the NBO atomic charges are slightly negative. Therefore, we should expect a stronger influence of the aluminum atoms on the catalyst process than of the oxygen atoms.

Adsorption of NO on the $Pd_4/Al_{14}O_{24}H_6$ cluster

After optimization of the positions of the four palladium atoms on the alumina surface, the NO molecule was adsorbed on the $Pd_4/Al_{14}O_{24}H_6$ cluster, keeping the atomic nuclei of $Pd_4/Al_{14}O_{24}H_6$ fixed in their previously optimized positions. Initially, four adsorption modes were tested: atop, bridge, di-σ and hollow. After optimization, all arrangements converged to the atop adsorption mode, with the NO unit bent to the alumina surface (Figure 4). Due to the unpaired electron of the NO molecule and considering the results found for the $Pd_4/Al_{14}O_{24}H_6$ cluster, four electronic spin states were calculated: doublet, quartet, sextet and octet. The electronic state of lowest energy depends on the position where NO adsorbs. The lowest energy electronic state for adsorption on the palladium atoms Pd(46) and Pd(47) is the doublet, while for adsorption on Pd(45) the lowest energy electronic state is the quartet. The most stable site for adsorption is Pd(47), as shown in Table 2, with adsorption energy of –25.6 kcal mol^{-1}, close to the experimental value of –27.2 kcal mol^{-1}.[18] The second site for adsorption is on Pd(45), with adsorption energy of –18.4 kcal mol^{-1} (all values corrected for BSSE, which amounts to 2-3 kcal mol^{-1} (see Tables S2 and S3)). The preferential site for adsorption of NO is on the palladium atom that is closer to the oxygen atoms, with the highest positive electronic charge. Therefore, our data indicate that the main parameter that determines the intensity of the interaction of NO with the palladium atoms is the charge on the corresponding palladium. More positive palladium atoms have higher ability to accept the σ electrons from the NO molecule, making the adsorption process stronger.

The lower Pd–N distance is found for adsorption on Pd(47), reflecting the stronger interaction of the NO molecule with this palladium atom. It is worth noting that the N–O distance after adsorption is high for adsorption on Pd(47), accompanying the order of the interaction energy, although close to the N–O distance for adsorption on Pd(46), probably reflecting the higher ability of this palladium atom (Pd(46)), due to its more negative charge, to donate electron back to the 2π* orbital of NO.

For all adsorption sites the NO molecule adsorbs in a bent geometry, in accordance with the literature.[24] The Pd–N–O angles varies between 131 and 136°. Adsorption in the bent arrangement favors overlap between the $d_z{}^2$ orbital on the palladium atom and the polarized 2π* orbital of NO.[52]

Reflecting the main type of interaction between the NO molecule and the supported palladium cluster, the total NBO charge density on the NO molecule is positive for all adsorption sites. Therefore, in general, there is charge transfer from the NO molecule to the palladium cluster, with higher values for charge transfer found for the adsorption sites Pd(45) and Pd(47). The palladium Pd(46), which has the most negative electronic charge when interacting with the alumina surface, has higher ability for electron back-donation, therefore making the NO not so positive.

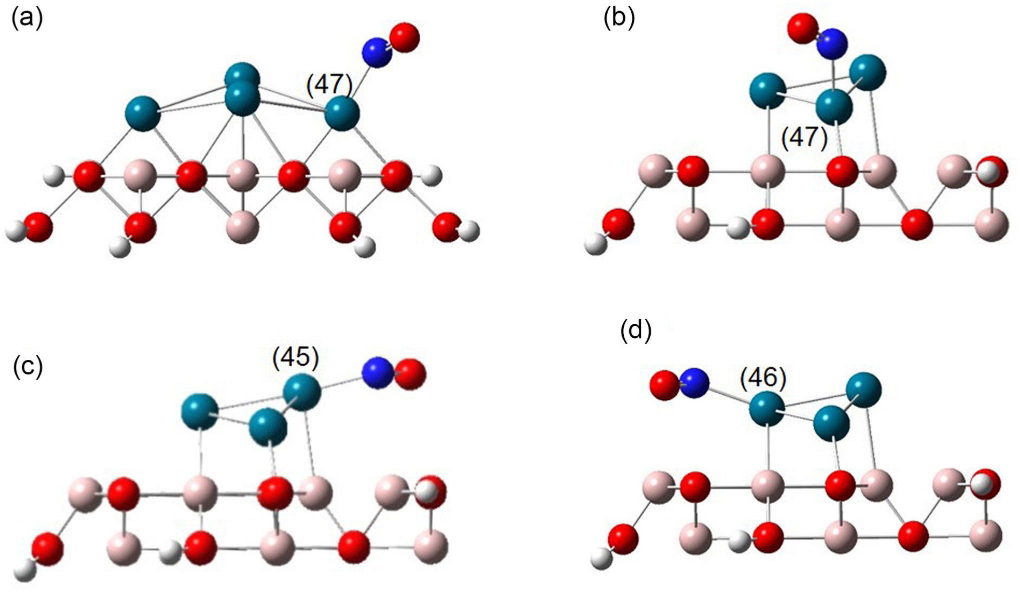

Figure 4. NO adsorption in different positions on the $Pd_4/Al_{14}O_{24}H_6$ cluster: (a and b) two lateral views for adsorption on Pd(47); (c) lateral view for adsorption on Pd(45); and (d) lateral view for adsorption on Pd(46).

Table 2. Geometrical parameters, adsorption energy ($E_{ad.}$, kcal mol^{-1}, corrected for BSSE) and charge density (e^-) on the Pd_4 cluster and on the nitric oxide (NO) for nitric oxide adsorbed on both Pd_4 supported on $Al_{14}O_{24}H_6$ and on the isolated Pd_4 with distorted geometry (distances in Å and bond angles in degrees)

	$NO/Pd_4/Al_{14}H_6O_{24}$			$NO/Pd_{4(distorted)}$		
	45	46	47	45	46	47
N–Pd / Å	2.012	2.100	1.904	1.843	1.900	1.865
N–O / Å	1.149	1.156	1.155	1.158	1.165	1.157
O–N–Pd / degree	135.69	131.12	130.62	131.24	112.69	131.81
$E_{ad.}$ / (kcal mol^{-1})	–18.39	–5.80	–25.60	–26.69	–25.45	–31.85
q_t $(Pd_4)_{(NBO)}$ / e^-	+0.380	+0.373	+0.308	+0.012	+0.019	+0.032
q_t $(NO)_{(NBO)}$ / e^-	+0.080	+0.029	+0.079	–0.012	–0.019	–0.032

$E_{ad.}$: adsorption energy; q_t: charge density.

Indeed, calculation of charge density with the alternative Merz-Kollman method indicates that NO adsorbed on Pd(46) becomes negatively charged.

Conclusions

The present computational study allowed us to derive relevant informations about the energetic, geometric and electronic parameters for adsorption of NO on palladium and on palladium supported on γ-alumina. The adsorption mode and adsorption energy for the NO molecule adsorbed on the Pd_4 clusters is dependent on the metal arrangement. When adsorbing on the planar Pd_4, the bridge adsorption mode is preferential, with adsorption energy of –41.2 kcal mol^{-1}. For adsorption on the tetrahedral arrangement of Pd_4 the atop adsorption form becomes the most stable, with adsorption energy of –30.6 kcal mol^{-1}. Atop adsorption on a distorted Pd_4 obtained by optimizing Pd_4 on the alumina surface has adsorption energy of –31.8 kcal mol^{-1}. The electron flux between the NO molecule and the Pd_4 cluster also depends on the adsorption mode, with electron transfer from the NO to the Pd cluster in the atop adsorption mode and in the opposite direction for adsorption in the bridge arrangement.

When interacting with the alumina surface, Pd_4 adsorbs with a strong deformation in the Pd_4 arrangement, leading to a structure with more dispersed palladium atoms and arrangement that is intermediate between the planar and the tetrahedral forms. The adsorption of Pd_4 on the alumina surface occurs with a high interaction energy (above 200 kcal mol^{-1}) and charge transfer from the palladium atoms to the alumina, particularly due to the strong interaction with the surface oxygen atoms, although palladium atoms directly placed over octahedral aluminum atoms become negatively charged.

NO adsorbs in an atop orientation on the $Pd_4/Al_{14}O_{24}H_6$ cluster, with adsorption energy of –25.6 kcal mol^{-1}. The NO molecule adsorbs preferentially on the palladium atoms with the highest positive charge, mainly due to the interaction via the σ electrons of NO. Charge transfer in this interaction mode is found from the NO molecule to the $Pd_4/Al_{14}O_{24}H_6$ cluster. However, when adsorbing on the more negative palladium atoms, charge back-donation to the NO molecule is also observed. Therefore, the effect of the alumina support on the palladium cluster is mainly to increase the dispersion of the palladium atoms, although with a slightly reduced energy for adsorption of NO.

Supplementary Information

Supplementary data are available free of charge at http://jbcs.sbq.org.br as PDF file.

Acknowledgments

The authors would like to thank CAPES for scholarship (L. M. P.) and the financial support given by CNPq (grant 478302/2012-6) and FAPERJ (grants E-26/201.302/2014 and E-26/111.708/2013) for research fellowship received by J. W. M. C.

References

1. Chinchilla, R.; Nájera, C.; *Chem. Rev.* **2014**, *114*, 1783.
2. Liao, F.; Lo, T. W. B.; Tsang, S. C. E.; *ChemCatChem* **2015**, *7*, 1998.
3. Saldan, I.; Semenyuk, Y.; Marchuk, I.; Reshetnyak, O.; *J. Mater. Sci.* **2015**, *50*, 2337.
4. Bagot, P. A. J.; *Mater. Sci. Technol.* **2004**, *20*, 679.
5. Belton, D. N.; Taylor, K. C.; *Curr. Opin. Solid State Mater. Sci.* **1999**, *4*, 97.
6. Heck, R. M.; Farrauto, R. J.; *Appl. Catal., A* **2001**, *221*, 443.
7. Ozensoy, E.; Hess, C.; Goodman, D. W.; *Top. Catal.* **2004**, *28*, 13.
8. Zaera, F.; *Chem. Soc. Rev.* **2014**, *43*, 7624.
9. Chen, X.; Cheng, Y.; Seo, C. Y.; Schwank, J. W.; McCabe, R. W.; *Appl. Catal., B* **2015**, *163*, 499.

10. Blaser, H.-U.; Indolese, A.; Schnyder, A.; Steiner, H.; Studer, M.; *J. Mol. Catal. A: Chem.* **2001**, *173*, 3.
11. Agostini, G.; Groppo, E.; Piovano, A.; Pellegrini, R.; Leofanti, G.; Lamberti, C.; *Langmuir* **2010**, *26*, 11204.
12. Lan, L.; Chen, S.; Cao, Y.; Gong, M.; Chen, Y.; *Catal. Sci. Technol.* **2015**, *5*, 4488.
13. Koshland Jr., D. E.; *Science* **1992**, *258*, 1861.
14. Weiss, B. M.; Iglesia, E.; *J. Catal.* **2010**, *272*, 74.
15. Hu, Y.; Griffiths, K.; Norton, P. R.; *Surf. Sci.* **2009**, *603*, 1740.
16. Hungría, A. B.; Fernández-García, M.; Anderson, J. A.; Martínez-Arias, A.; *J. Catal.* **2005**, *235*, 262.
17. Neyertz, M.; Volpe, M.; Perez, D.; Costilla, I.; Sanchez, M.; Gigola, C.; *Appl. Catal., A* **2009**, *368*, 146.
18. Wang, C.-B.; Yeh, T.-F.; Lin, H.-K.; *J. Hazard. Mater.* **2002**, *92*, 241.
19. Auvray, X.; Olsson, L.; *Appl. Catal., B* **2015**, *168-169*, 342.
20. Kaneeda, M.; Iizuka, H.; Hiratsuka, T.; Shinotsuka, N.; Arai, M.; *Appl. Catal., B* **2009**, *90*, 564.
21. Begum, P.; Gogoi, P.; Mishra, B. K.; Deka, R. C.; *Int. J. Quantum Chem.* **2015**, *115*, 837.
22. Piotrowski, M. J.; Piquini, P.; Zeng, Z.; da Silva, J. L. F.; *J. Phys. Chem. C* **2012**, *116*, 20540.
23. Lacaze-Dufaure, C.; Roques, J.; Mijoule, C.; Sicilia, E.; Russo, N.; Alexiev, V.; Mineva, T.; *J. Mol. Catal. A: Chem.* **2011**, *341*, 28.
24. Grybos, R.; Benco, L.; Bučko, T.; Hafner, J.; *J. Comput. Chem.* **2009**, *30*, 1910.
25. Grybos, R.; Benco, L.; Bučko, T.; Hafner, J.; *J. Chem. Phys.* **2009**, *130*, 104503.
26. Geng, L.; Han, L.; Cen, W.; Wang, J.; Chang, L.; Kong, D.; Feng, G.; *Appl. Surf. Sci.* **2014**, *321*, 30.
27. Duarte, H. A.; Salahub, D. R.; *Top. Catal.* **1999**, *9*, 123.
28. Bertin, V.; del Angel, G.; Mora, M. A.; Poulain, E.; Olvera, O.; López-Rendón, R.; *J. Mex. Chem. Soc.* **2008**, *52*, 93.
29. Zeng, Z.-H.; da Silva, J. L. F.; Li, W.-X.; *Phys. Chem. Chem. Phys*. **2010**, *12*, 2459.
30. Kacprzak, K. A.; Czekaj, I.; Mantzaras, J.; *Phys. Chem. Chem. Phys*. **2012**, *14*, 10243.
31. Valero, M. C.; Raybaud, P.; Sautet, P.; *J. Catal*. **2007**, *247*, 339.
32. Chang, J. R.; Chang, S.-L.; Lin, T. B.; *J. Catal.* **1997**, *169*, 338.
33. Carneiro, J. W. M.; Cruz, M. T. M.; *J. Phys. Chem. A* **2008**, *112*, 8929.
34. Márquez, A. M.; Sanz, J. F.; *Appl. Surf. Sci.* **2004**, *238*, 82.
35. Alvarez, L. J.; Sanz, J. F.; Capitán, M. J.; Centeno, M. A.; Odriozola, J. A.; *J. Chem. Soc., Faraday Trans.* **1993**, *89*, 3623.
36. Wyckoff, R. W. G.; *Crystal Structures*; John Wiley Interscience Publishers: New York, 1968.
37. The electronic ground state computed for Al_xO_y cluster is dependent on the Al_xO_y arrangement. However, computations of single-point MP2/6-31g(d) relative energies (not reported) confirm the singlet state as the ground state for all Al_xO_y forms.
38. van Duijneveldt, F. B.; van Duijneveldt-van de Rijdt, J. G. C. M.; van Lenthe, J. H.; *Chem. Rev.* **1994**, *94*, 1873.
39. Lopes, J. F.; Rocha, W. R.; dos Santos, H. F.; de Almeida, W. B.; *J. Braz. Chem. Soc.* **2010**, *21*, 887.
40. Frisch, M. J.; Trucks, G. W.; Schlegel, H. B.; Scuseria, G. E.; Robb, M. A.; Cheeseman, J. R.; Montgomery, Jr., J. A.; Vreven, T.; Kudin, K. N.; Burant, J. C.; Millam, J. M.; Iyengar, S. S.; Tomasi, J.; Barone, V.; Mennucci, B.; Cossi, M.; Scalmani, G.; Rega, N.; Petersson, G. A.; Nakatsuji, H.; Hada, M.; Ehara, M.; Toyota, K.; Fukuda, R.; Hasegawa, J.; Ishida, M.; Nakajima, T.; Honda, Y.; Kitao, O.; Nakai, H.; Klene, M.; Li, X.; Knox, J. E.; Hratchian, H. P.; Cross, J. B.; Bakken, V.; Adamo, C.; Jaramillo, J.; Gomperts, R.; Stratmann, R. E.; Yazyev, O.; Austin, A. J.; Cammi, R.; Pomelli, C.; Ochterski, J. W.; Ayala, P. Y.; Morokuma, K.; Voth, G. A.; Salvador, P.; Dannenberg, J. J.; Zakrzewski, V. G.; Dapprich, S.; Daniels, A. D.; Strain, M. C.; Farkas, O.; Malick, D. K.; Rabuck, A. D.; Raghavachari, K.; Foresman, J. B.; Ortiz, J. V.; Cui, Q.; Baboul, A. G.; Clifford, S.; Cioslowski, J.; Stefanov, B. B.; Liu, G.; Liashenko, A.; Piskorz, P.; Komaromi, I.; Martin, R. L.; Fox, D. J.; Keith, T.; Al-Laham, M. A.; Peng, C. Y.; Nanayakkara, A.; Challacombe, M.; Gill, P. M. W.; Johnson, B.; Chen, W.; Wong, M. W.; Gonzalez, C.; Pople, J. A.; *Gaussian 03*, Revision B.04; Gaussian, Inc., Pittsburgh, 2003.
41. Becke, A. D.; *J. Chem. Phys.* **1992**, *96*, 2155.
42. Lee, C.; Yang, W.; Parr, R. G.; *Phys. Rev. B: Condens. Matter Mater. Phys.* **1988**, *37*, 785.
43. Hay, P. J.; Wadt, W. R.; *J. Chem. Phys.* **1985**, *82*, 270.
44. Dunning Jr., T. H.; Hay, P. J. In *Modern Theoretical Chemistry*; Schaefer III, H. F., ed.; Plenum: New York, 1976.
45. Clark, T.; Chandrasekhar, J.; Spitznagel, G. W.; Schleyer, P. R.; *J. Comput. Chem.* **1983**, *4*, 294.
46. Liu, X.; Tian, D.; Ren, S.; Meng, C.; *J. Phys. Chem. C* **2015**, *119*, 12941.
47. Loffreda, D.; Simon, D.; Sautet, P.; *Chem. Phys. Lett.* **1998**, *291*, 15.
48. Hansen, K. H.; Sljivancanin, Z.; Hammer, B.; Laegsgaard, E.; Besenbacher, F.; Stensgaard, I.; *Surf. Sci.* **2002**, *496*, 1.
49. Cruz, M. T. M.; Carneiro, J. W. M.; Aranda, D. A. G.; Bühl, M.; *J. Phys. Chem. C* **2007**, *111*, 11068.
50. Oemry, F.; Escano, M. C.; Kishi, H.; Kunikata, S.; Nakanishi, H.; Kasai, H.; Maekawa, H.; Osumi, K.; Tashiro, Y.; *J. Nanosci. Nanotechnol.* **2011**, *11*, 2844.
51. Gomes, J. R. B.; Lodziana, Z.; Illas, F.; *J. Phys. Chem. B* **2003**, *107*, 6411.
52. Viñes, F.; Desikusumastuti, A.; Staudt, T.; Görling, A.; Libuda, J.; Neyman, K. M.; *J. Phys. Chem. C* **2008**, *112*, 16539.

Submitted: January 14, 2016